Enhanced thymic selection of FoxP3$^+$ regulatory T cells in the NOD mouse model of autoimmune diabetes

Markus Feuerer*, Wenyu Jiang*, Phillip D. Holler*, Ansuman Satpathy*, Christopher Campbell*, Molly Bogue†, Diane Mathis*‡, and Christophe Benoist*‡

*Section on Immunology and Immunogenetics, Joslin Diabetes Center, Department of Medicine, Brigham and Women's Hospital, Harvard Medical School, Boston, MA 02215; and †The Jackson Laboratory, Bar Harbor, ME 04609

Contributed by Christophe Benoist, September 25, 2007 (sent for review September 6, 2007)

FoxP3$^+$CD4$^+$ regulatory T cells (Tregs) play a key role in the maintenance of peripheral self-tolerance, and it has been suggested that diabetes-susceptible nonobese diabetic (NOD) mice are defective in the generation and numbers of Tregs. We found thymic selection of Tregs to be under genetic control. Fetal thymic organ cultures on the NOD background required 3- to 10-fold more antigen than corresponding cultures on the B6 background for optimal induction of Tregs, but once the threshold for induction was reached the NOD background yielded close to 10-fold more Tregs. This increased selection of Tregs was also found in nontransgenic NOD mice in fetal through adult stages. This trait did not map to the MHC, *idd3*, or the chromosome 3 (*Chr3*) regions that control clonal deletion, but mainly to two regions on *Chr1* and *Chr11*. Thus, NOD mice do not have a global defect in the generation or maintenance of Tregs; if anything, they show the opposite.

genetic | lineage commitment | thymus

Regulatory T cells (Tregs) play a key role in the maintenance of peripheral self-tolerance (1). It was found that such cells express the forkhead/winged helix transcription factor FoxP3 (2–4), and that deficiencies in FoxP3 underlie the lymphoproliferation and multiorgan autoimmunity in *scurfy* mutant mice and human patients with immunodysregulation polyendocrinopathy and enteropathy, X-linked syndrome (5). FoxP3-GFP reporter mice, as well as intracellular staining for FoxP3, revealed that 60–88% of FoxP3$^+$ cells express high levels of CD25, depending on the tissue localization (6). A distinct gene-expression signature is also characteristic of Tregs (6–8).

Tregs in normal mice are generated in the thymus, but how immature thymocytes are selected into this alternative lineage remains a question of central interest. The repertoire of Tregs is enriched in autoreactive T lymphocytes. In some experimental systems, Treg differentiation appeared to be induced when the T cell receptor (TCR) on immature thymocytes was engaged by agonist ligands (9, 10). Alternatively, some investigators have proposed that the observed high frequency of Tregs resulting from recognition of cognate ligand may reflect a higher resistance of Treg versus conventional CD4$^+$ T cell thymic precursors to clonal deletion (11, 12). Still others have suggested that Treg selection may be favored in particular thymus stromal niches (13). In addition, mature CD4$^+$ T cells from peripheral lymphoid organs can be converted to FoxP3 positivity by exposure to TGF-β (14) or chronic stimulation by agonist peptide (15).

The activity or inactivity of Tregs plays an important role in controlling the development of autoimmune diabetes in the nonobese diabetic (NOD) mouse model (16): transfer of Tregs can protect the recipients from diabetes, whether they be NOD mice or TCR transgenic systems derived from NOD (17–19), and genetic deficiencies that reduce Treg numbers or activity that lead to accelerated diabetes (17, 18). It has been suggested that NOD mice have a generalized defect in their ability to generate effective numbers of Tregs, with a percentage of CD4$^+$CD25$^+$ T cells lower that of other autoimmunity-resistant mouse strains (17, 20, 21), and other studies report age-dependent declines in Treg-suppressive activity in NOD mice (22–24). Here, we have analyzed genetic variation in the thymic generation of Tregs, focusing on NOD and the diabetes-resistant MHC-matched B6.H2^{g7} as well as a panel of other inbred strains. To our surprise, the NOD background proved superior at generating Tregs in the thymus, whether in response to agonist ligands or in unmanipulated conditions.

Results

Generation of Tregs in Fetal Thymus Organ Cultures (FTOCs). As mentioned above, there is a contradiction between results from certain experimental systems that suggested direct induction of Treg differentiation by TCR engagement with agonist ligands (9, 10) versus other systems where preferential survival of Tregs could account for an apparent increase in self-reactive Treg thymocytes upon agonist exposure, without an actual induction of differentiation (11, 12, 25). To address this contradiction, we investigated the generation of Tregs in FTOCs, using embryonic day 15 (E15) thymic lobes from timed matings of BDC2.5/NOD mice. The BDC2.5 mouse line was derived from a CD4$^+$ T cell clone, restricted by the NOD MHC class II A^{g7} molecule, and specific for an unknown β cell antigen (26).

Neither FoxP3 RNA nor the corresponding protein could be detected at FTOC initiation (data not shown). Cultures were incubated for 7 days, and the appearance of Tregs was monitored by staining for CD25 and FoxP3 among CD4 single-positive (CD4SP) thymocytes. In the NOD FTOCs ≈4% of the CD4SPs were Tregs, a value comparable with that of normal CD4SP thymocytes (Fig. 1*A Left*). Thus, the thymus is fully competent to produce this subset of Tregs in an autonomous fashion. Fewer Tregs were generated in lobes from BDC2.5/NOD embryos, indicating that the BDC2.5 TCR is less compatible with selection into the Treg pathway than is the diverse repertoire of NOD mice (Fig. 1*A Center*), as commonly observed with TCR transgenic mice. On the other hand, a robust Treg population (10–20% of CD4SPs) was induced by addition of 10 ng/ml BDC2.5 mimotope peptide agonist (Fig. 1*A Right*). In peptide titrations, the proportion of Tregs among CD4SPs increased from <1% (no

Author contributions: M.F., W.J., P.D.H., A.S., C.C., D.M., and C.B. designed research; M.F., W.J., P.D.H., A.S., and C.C. performed research; M.B. contributed new reagents/analytic tools; M.F., W.J., P.D.H., A.S., and C.C. analyzed data; and M.F., D.M., and C.B. wrote the paper.

The authors declare no conflict of interest.

Abbreviations: NOD, nonobese diabetic; Treg, regulatory T cell; FTOC, fetal thymus organ culture; Chr(*n*), chromosome number; TCR, T cell receptor; CD4SP, CD4 single-positive; DP, double-positive; QTL, quantitative trait loci; E(*n*), embryonic day.

‡To whom correspondence should be addressed. E-mail: cbdm@joslin.harvard.edu.

This article contains supporting information online at www.pnas.org/cgi/content/full/0708899104/DC1.

IMMUNOLOGY

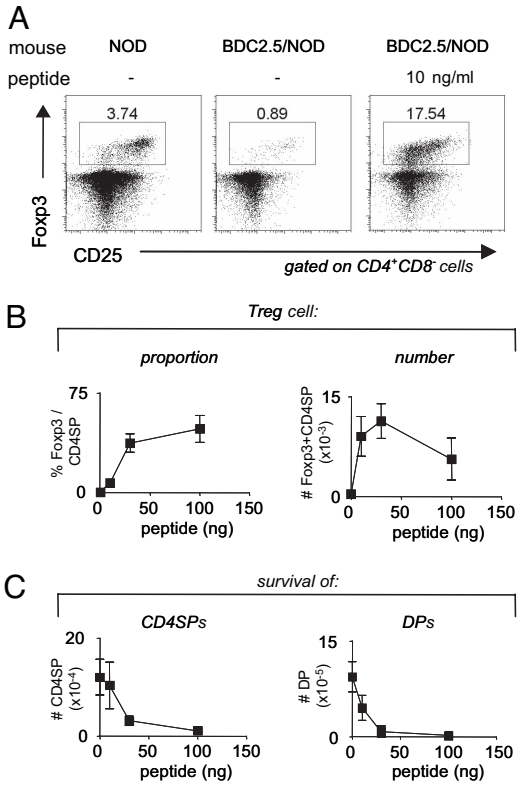

Fig. 1. Treg induction in BDC2.5/NOD FTOC system. BDC2.5/NOD and NOD FTOCs were cultured for 7 days. BDC2.5/NOD lobes were supplemented with BDC-specific mimotope peptide. (*A*) Induction of Foxp3$^+$ Tregs in FTOCs from NOD and BDC2.5/NOD mice either with or without peptide. Cells were gated for CD4$^+$CD8$^-$. Numbers show the percentage of Foxp3$^+$ Tregs per CD4SP. Representative dot plots are shown. (*B*) BDC2.5/NOD FTOCs were cultured with different peptide concentrations. Proportion and absolute number of Foxp3$^+$ Tregs cells per CD4SP are displayed. (*C*) Total number of CD4SP and DP cells from the cultures described in *B* are shown as a measure for deletion (survival). Mean and SD of four independent experiments with three to six pooled FTOCs per peptide concentration and experiment are shown.

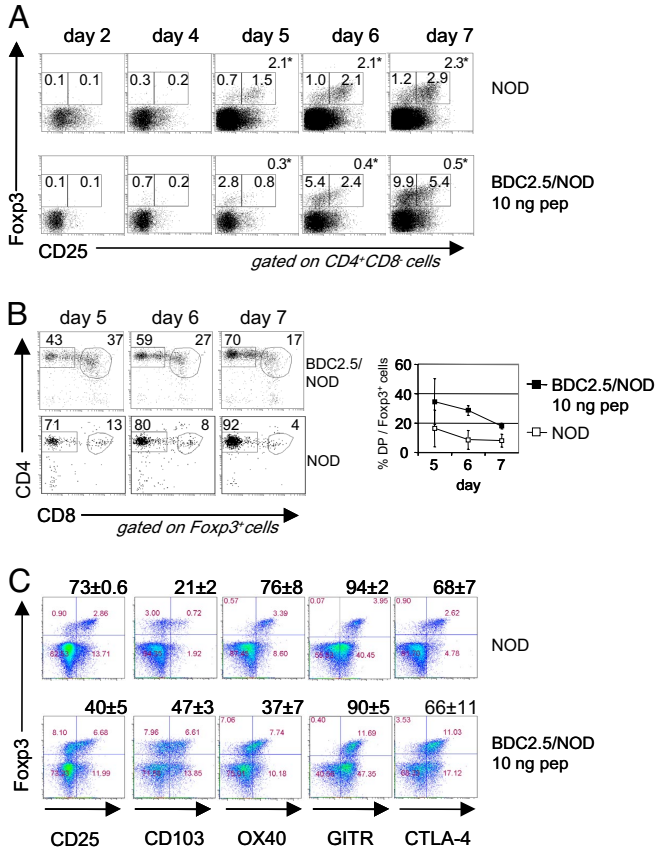

Fig. 2. Differences in peptide-induced and naturally selected Tregs. BDC2.5/NOD and NOD FTOCs were cultured in parallel for 2–7 days. BDC2.5/NOD lobes were supplemented with 10 ng of BDC-specific peptide. (*A*) Cells were gated for CD4$^+$CD8$^-$. Bold numbers show percentage of Foxp3$^+$ and CD25$^+$ or CD25$^-$ Tregs. *, Ratio of CD25$^+$/CD25$^-$ of Foxp3$^+$ T cells. Three to four FTOCs per day and group were pooled and one representative experiment of two is shown. (*B*) (*Left*) BDC2.5/NOD FTOCs were harvested and gated for Foxp3$^+$ cells. Percentage of CD4SP and DP are shown. (*Right*) Percentage of DP among Foxp3$^+$ cells. Filled symbols are BDC2.5/NOD FTOCs; open symbols are NOD FTOCs. Representative dot plots and mean and SD of three independent experiments are shown. (*C*) FTOCs were cultured for 7 days and gated for CD4SP cells. Canonical Treg-specific proteins were stained and shown in bold are the percentage of Foxp3 DP Tregs. Representative dot plots and mean and SD of three experiments are shown.

peptide) to >50% (100 ng/ml peptide; Fig. 1*B Left*). This increase reflected a true induction of Tregs, as their total number also increased >20-fold at the optimal peptide dose (30 ng) (Fig. 1*B Right*). The peptide titration also reproduced the differential sensitivity of conventional and regulatory CD4SP precursors to agonist-induced deletion: Tregs were induced at a dose of peptide that resulted in the loss of conventional CD4SPs and of CD4, CD8 double-positive (DP) thymocytes (Fig. 1*C*). Thus, true induction of Treg differentiation occurs in the BDC2.5 system, in a range of agonist stimulation where a certain degree of negative selection also occurred.

We then asked whether the agonist-induced Tregs in BDC2.5/NOD FTOC had an origin or phenotypic characteristics different from those of Tregs "naturally" selected in NOD FTOCs. Comparing the kinetics of Treg generation between NOD and peptide-stimulated BDC/NOD FTOCs revealed no differences between the two groups. The first evidence of FoxP3 expression was simultaneously detected on day 4 (Fig. 2*A*). There has been some debate as to the stage in thymocyte differentiation where Tregs first appear. They could potentially differentiate from immature DP precursors, as conventional SPs do, or later from committed CD4SPs that have migrated into the medulla (6, 13). The kinetic analysis revealed that DP FoxP3$^+$ thymocytes were induced in the BDC2.5/NOD FTOCs, in highest frequency at day 5 of the culture, and decline as a fraction of the total FoxP3 population from ≈35% at day 5 to 18% by day 7, with a corresponding increase in CD4SPs FoxP3$^+$ thymocytes (Fig. 2*B Left* and *Right*). NOD FTOCs showed a parallel evolution, albeit with fewer DPs within the FoxP3$^+$ populations (Fig. 2*B Right*). These data are consistent with a scenario wherein self-reactive cells enter the Treg lineage at the DP thymocytes stage, followed by a transition to CD4SP compartment, although some conversion of committed CD4SPs may also occur.

Close inspection of the data in Fig. 2*A* revealed that the FoxP3$^+$ Tregs induced in the BDC2.5/NOD cultures had a different distribution of CD25 expression, with a predominance of CD25$^-$ cells. Therefore, we compared the distribution of some of the hallmark molecules of Tregs on naturally selected and agonist-induced Treg thymocytes. Differences were detected for CD103 and OX40 (CD134) (Fig. 2*C*). GITR and CTLA4 expression showed no marked divergence in the two groups.

Genetic Differences in Treg Generation. Given the generally accepted notion that NOD mice have some kind of defect in Tregs, we asked whether the genetic variation between the NOD strain and the diabetes-resistance C57BL/6 (B6) reference strain might

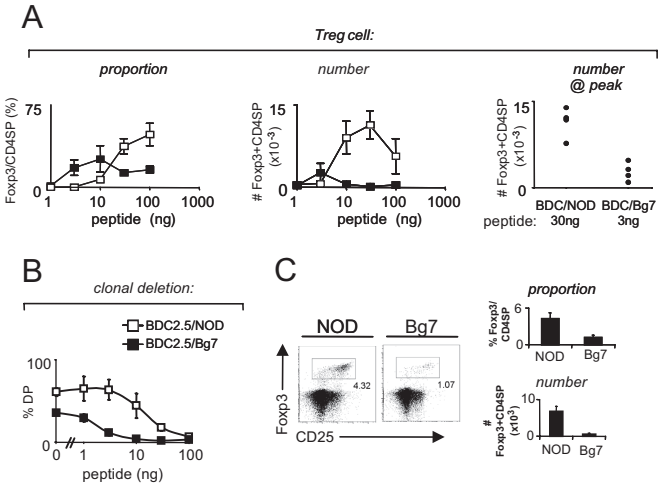

Fig. 3. Strain differences between NOD and Bg7 in Treg induction. FTOCs were cultured for 7 days. FTOCs cultures were performed in parallel with embryos from BDC2.5/NOD (open symbols) mice and BDC2.5/Bg7 (filled symbols) mice and supplemented with different concentrations of BDC-specific peptide. (*A*) (*Left* and *Middle*) Percentage and absolute number of Foxp3$^+$ Tregs per CD4SP. Mean and SD of four independent experiments with each three to six pooled FTOC lobes per concentration and group are shown. (*Right*) Number at peak shows absolute number of Foxp3$^+$ cells at the peptide concentration with a maximum of Treg induction (3 ng for BDC/Bg7 and 30 ng for BDC/NOD). Presented are four individual experiments. (*B*) Deletion based on percentage of DP cells. (*C*) Nontransgenic FTOC experiments from NOD mice and Bg7 mice. (*Left*) Numbers show percentage of Foxp3$^+$ Tregs per CD4SP of representative dot plots. (*Right*) Percentage and absolute number of Foxp3$^+$ Tregs per CD4SP and mean and SD of three independent experiments with three to five FTOCs per group and experiment are shown.

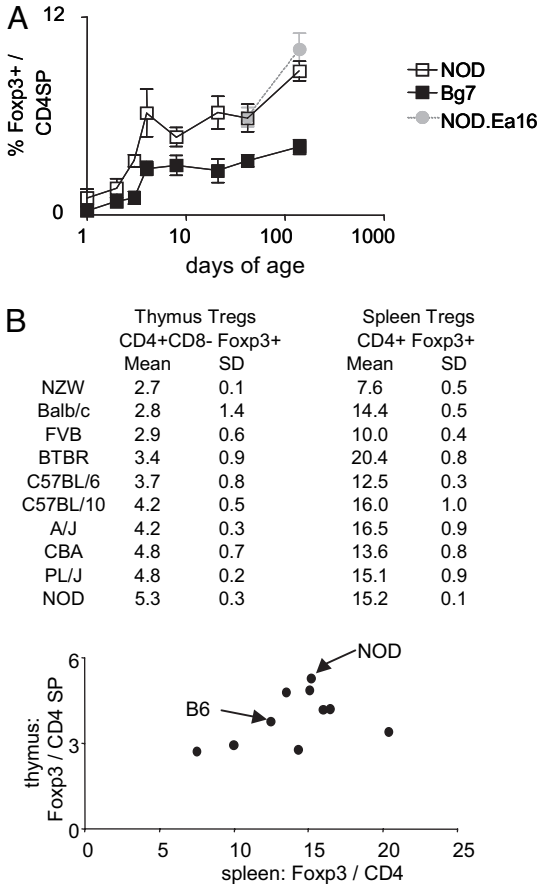

Fig. 4. Comparison of *ex vivo* T cells from NOD and Bg7 mice. Thymus and spleen cells were isolated and stained for CD4, CD8, CD25, Foxp3, and TCR-β-chain. Percentage of Foxp3$^+$ Tregs per CD4SP was analyzed. (*A*) Thymi from NOD mice (open symbols), NOD.Ea16 mice (gray symbols, dashed line), and Bg7 mice (black symbols) were isolated at different days after birth, and percentage of Foxp3$^+$ per CD4SP T cells was analyzed. Mean and SD of 3–11 mice per group and time point are shown. (*B*) Broad screen of Tregs among inbred mouse strains. Thymus and spleen from 10 inbred mouse strains were analyzed. Mean percentage of CD4$^+$Foxp3$^+$ Tregs and SD are shown. Three mice per strain were analyzed. Mean values from spleen and thymus were plotted, and NOD and B6 mice are highlighted.

influence the propensity for generating Tregs in FTOCs. Parallel transgenic lines were used, the same BDC2.5 transgenes being crossed onto the NOD or congenic B6.H2^{g7} (Bg7) backgrounds (27), which share the selecting MHC class II A^{g7} molecule but differ in all non-MHC genes. FTOCs were performed with embryos from each of the two strains, and the proportion and numbers of FoxP3$^+$CD4$^+$ Tregs generated were compared, as well as the extent of overall clonal deletion (reflected by the proportion of remaining DP cells). The titration of agonist peptide revealed very different responses on the two genetic backgrounds (Fig. 3): BDC2.5/Bg7 lobes were more susceptible to clonal deletion than BDC2.5/NOD lobes were, confirming our previous findings (28), and generated more Tregs at low agonist concentrations (Fig. 3*A*). On the other hand, when matched for the intensity of clonal deletion, NOD FTOCs were actually superior at generating Tregs, as both proportion (Fig. 3*A Left*) and absolute number [Fig. 3*A Center* and supporting information (SI) Table 1]. The optimal induction occurred in different windows of peptide concentrations for the two strains. Tregs were induced in BDC2.5/Bg7 lobes with 3- to 10-fold less peptide, the peak number of Tregs being distinctly higher on the NOD background, a consistent observation over four experiments (Fig. 3*A Right*).

To determine whether the differences in Treg induction between the NOD and B6.H2g7 (Bg7) backgrounds reflected a general feature or were restricted to the BDC2.5 TCR transgenic system, we examined FTOCs from nontransgenic embryos. Here again, the proportion of FoxP3$^+$ cells among CD4SPs, and their total numbers, was higher in NOD versus Bg7 (Fig. 3*C*).

The surprisingly greater ability of NOD FTOCs to generate Tregs raised the question of whether these observations resulted merely from an artifact of *in vitro* culture. Thus, we analyzed Tregs *ex vivo* from NOD and Bg7 mice, staining CD4$^+$ T cells from several lymphoid organs for FoxP3 and CD25. A detailed time-course analysis of Treg appearance in the thymus was performed, which showed their proportion among CD4SPs to increase over time in both strains, consistent with a previous report (13); this proportion was consistently higher for NOD mice at all time points tested, in neonatal, infant, or adult mice (Fig. 4*A*). This increase was not an artifact of NOD's autoimmune attack to the pancreas, because it was also observed in NOD.Eα16 mice, genetically identical to NOD animals, but protected from insulitis by an MHC class II *Ea* transgene (29).

NOD and B6 are just two mouse strains, and differences observed above could be caused by an extreme representation in either strain. To this end, we analyzed thymic and splenic in 10 mouse strains from the Mouse Phenome Project (30) (all in 5- to 6-week-old mice, in triplicate). A wide distribution of proportions was observed for Foxp3$^+$ cells among thymic CD4$^+$CD8$^-$ SPs (from 2.7 to 5.3%; Fig. 4*B*). In keeping with the results above, NOD and B6 mice were on the high and low ends of that distribution, respectively, but still within the normal range [consistent with a prior study (31), and with a broader 33-strain analysis performed earlier with a CD25^{hi} phenotype as an indicator of Tregs (SI Fig. 6)]. The proportion of Tregs in spleen

generally correlated with thymic proportions, although there was some reordering of the rankings: for instance, the relative proportion and ranking for B6 mice increased. These results indicate that B6 and NOD mice are not extreme outlyers among mouse strains and suggest that the proportion of peripheral Tregs is influenced by the thymic output, but that their homeostatic control may also obey independent genetic cues.

Overall, NOD mice show no dearth of Tregs; if anything, they show the opposite.

Where Does the Efficient Treg Generation of NOD Mice Map? Given the demonstration that Tregs were generated more efficiently in the thymus of NOD than Bg7 mice, we sought to identify the origin of this difference.

The first issue to resolve was whether the difference was intrinsic to the differentiating thymocytes or to the thymic stroma. To this end, criss-cross reaggregation experiments were performed, where E15 DN T cell precursors were transferred into lobes depleted of their own lymphoid precursors by deoxyguanosine pretreatment. After culture, thymocytes derived from donor precursors were identified via the CD45 allotype marker (Fig. 5*A*). Higher proportions and numbers of Tregs were generated from NOD precursors, irrespective of the strain origin of the host lobe. Thus, T cell-intrinsic differences accounted for the strain differences in Treg selection.

The *Idd3* locus has been linked with higher IL-2 production and Treg number in the periphery (32). We wondered whether the *idd3* locus might also be responsible for the differences in Treg generation between NOD and B6 mice. FTOCs from NOD.*idd3*$^{b/b}$ congenic mice demonstrated that the *idd3* locus was not responsible for this difference (Fig. 5*B*).

We next asked which genetic loci contribute to this difference, anticipating that this information might also lead to new insights into the genetic control of Treg differentiation. To address this question, we intercrossed NOD and Bg7 mice to yield (NODxBg7) F_1 and F_2 embryos and measured FoxP3 and CD25 expression on the CD4SP thymocytes. Compared with their parental NOD and Bg7 counterparts, F_1 embryos demonstrated an intermediate percentage of Tregs; F_2 embryos, which carried random combinations of alleles from the parental backgrounds, showed a broad range of FoxP3$^+$ cells (Fig. 5*C*).

A genomewide scan was performed on the DNA from 137 of these (NODxBg7) F_2 embryos, genotyping 106 SNPs that distinguish the NOD and B6 genomes (average spacing of 25 Mb). Marker-trait association was performed with R/qtl software, with permutation analysis to estimate thresholds for genome-wide significance. Peaks of significant association were detected on chromosome 1 (*Chr1*) (100–180 Mb) and *Chr11* (between 100 Mb and the telomere; Fig. 5 *D* and *E*). At both loci, the NOD-derived allele was associated with a higher Treg proportion, essentially dominant for the *Chr1* quantitative trait loci (QTL), and additive for the QTL on *Chr11* (SI Fig. 7). Together, these two QTLs account for 28.9% of the variance, which represents a very substantial proportion in such analyses. Thus, the differential selection of Tregs in NOD and B6 thymi is under traceable Mendelian control and maps away from loci that condition the basic efficacy of clonal deletion and deviation, or the maintenance of Tregs in the periphery.

Discussion

The results presented herein demonstrate that the thymic selection of Tregs is under genetic control and also lead to an unexpected perspective on Tregs in the autoimmunity-prone NOD mouse, with more effective Treg selection in the thymus than in the reference diabetes-resistant strain, B6. These data imply that defective selection of Tregs is not a major component of diabetes susceptibility in the NOD mouse.

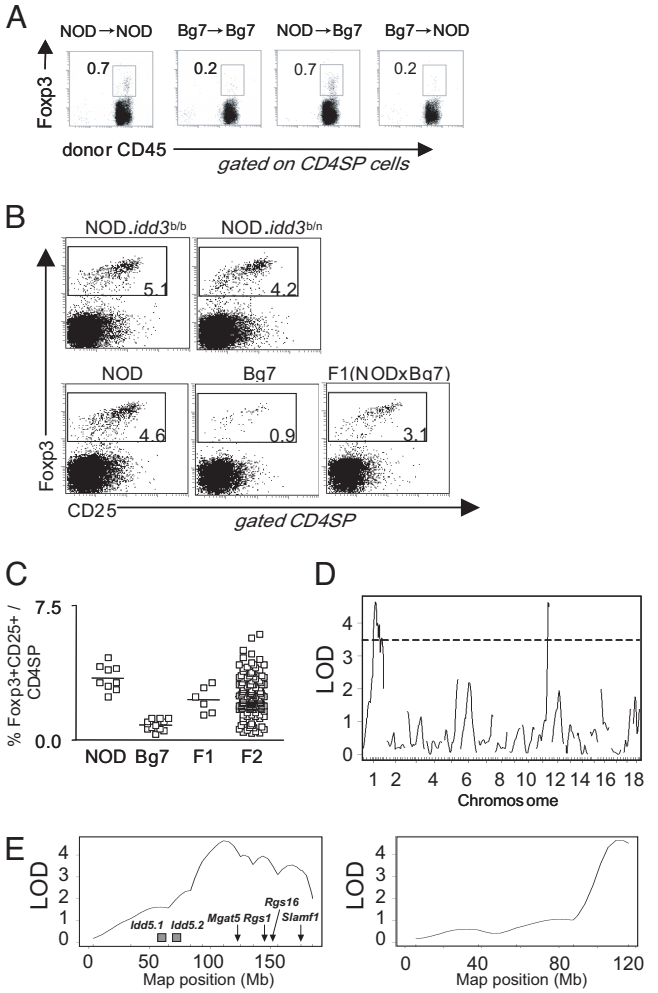

Fig. 5. Two genomic regions promote an enhanced selection of Tregs in NOD. (*A*) Repopulation thymus organ culture revealed that differences in Treg selection were intrinsic to the developing T cells. DN thymocytes from E15.5 embryos from the two strains were repopulated into deoxyguanosine-treated FTOC lobes from NOD or Bg7 mice. Donor cells could be discriminated by differences in expression of CD45 (NOD, CD45.1; Bg7, CD45.2). Numbers show the percentage of Foxp3$^+$ Tregs per CD4SP. One of two independent experiments is shown. (*B*) FTOCs from NOD.*idd3*$^{b/b}$, NOD.*idd3*$^{b/n}$ congenic, and NOD, Bg7, and F_1 (NODxBg7) mice are shown. Representative dot plots from three to five FTOCs are shown. (*C*) NOD, Bg7, F_1, and F_2 FTOCs were cultured for 7 days, and expression of Foxp3$^+$CD25$^+$ Tregs per CD4SP was measured. (*D*) Logarithm of odds plots for the FTOC/F2 cohorts are shown. Dotted line represents level of significance ($P < 0.05$). (*E*) Linkage maps of *Chr1* (*Left*) and *Chr11* (*Right*).

Our initial studies focused on Treg differentiation in FTOCs to assure that all differences were purely thymus-derived and to permit greater experimental flexibility. The results confirmed that the thymus is autonomously capable of generating Tregs, and the good match between relative numbers in FTOCs and neonatal mice indicates that FTOCs can serve as a valid experimental model in which to study the selection of Tregs. Previous reports using TCR transgenic mice coexpressing cognate ligand in the thymus suggested that high-affinity engagement of a self-ligand by the transgenic TCR induced a signal that could commit thymocytes to the Treg lineage (9, 10). Alternately, we and others have argued that the higher frequency of Tregs in the thymus of other TCR/Ag double-transgenic mice could be entirely explained by selective survival of Tregs (11, 12). Here, we found evidence of both scenarios in FTOCs from BDC2.5

TCR transgenic mice. FoxP3$^+$ cells were certainly more resistant to an agonistic stimulus that induced clonal deletion in immature thymocytes, particularly at high antigen concentrations, but, at lower concentrations, true induction of FoxP3$^+$ Tregs was clearly evident as well.

It had not been clear whether Tregs induced experimentally by agonist ligand are phenotypically and functionally the same as the "naturally" selected Tregs generated in the thymus of a normal mouse. Comparing naturally selected Tregs from nontransgenic mice with agonist-induced transgenic Tregs in FTOCs showed their kinetic of generation to be quite similar, although the agonist-induced FoxP3$^+$ cells were enriched in DP thymocytes (up to 40% of all FoxP3$^+$ cells). This difference is consistent with the notion that channeling of thymocytes into the Treg lineage may occur at different stages of differentiation depending on the thymus location in which the TCR self-agonist is encountered (33). In the FTOC system, immature DPs encounter the agonist peptide in the cortex of the developing cultures, whereas some of the Tregs selected in a normal thymus may depend more on presentation of self-antigens in the medulla. Several markers typical of Tregs proved differentially expressed in Tregs selected by the two modes: agonist-induced Tregs displayed less CD25 and OX40 and more CD103.

One might propose that Tregs are a heterogeneous population, harboring TCRs with a spectrum of affinities/avidities for self-antigens, and with a range of phenotypic characteristics that reflect this spectrum. The CD103$^+$ CD25^{lo} OX40^{lo} phenotype might denote Tregs elicited by a high-affinity ligand, whereas the CD103$^-$ CD25^{hi} Ox40^{hi} phenotype might be that of Tregs with lower affinity for self-ligand. Thus, the phenotypic and functional differences observed in peripheral Treg populations (7) could reflect differences in their encounter of high-affinity ligand during thymic selection, potentially continued in the periphery.

When the generation of Tregs on the NOD and B6 backgrounds were compared, clear differences in sensitivity were detected. As reported (28, 34), the NOD background confers a relative resistance to clonal deletion and also to clonal deviation toward the CD8$\alpha\alpha$ and Treg lineages (35). BDC2.5/NOD FTOCs needed 3- to 10-fold more antigen than BDC2.5/Bg7 embryos for optimal induction of Tregs. But, once the threshold for induction was reached, the NOD background was much more effective, with close to 10-fold higher yields of Tregs at comparable levels of clonal deletion. This greater propensity was also manifest in the absence of agonist stimulation in FTOCs and thymi of nontransgenic NOD mice at a variety of age groups, whether or not they were subject to autoimmune insulitis. An increased selection of Tregs thus appears to be a fundamental characteristic of the NOD genome, with predominant roots on *Chr1* and *Chr11*. Importantly, these regions are different from the QTL that controls the overall resistance to clonal deletion and clonal deviation, which maps to *Chr3* (28, 35) and are independent of the *idd3* region (32).

This genetic variation is not limited to NOD and B6 mice. A wide range of frequencies of FoxP3$^+$ cells was observed in the thymus of young adult mice of the Phenome panel. It will be of interest to ascertain whether other elements, beyond those uncovered in the strain combination studies here, control Treg selection. Yamanouchi *et al.* (32) have reported a correlation between the diabetes-susceptible NOD haplotype at the *Il2* locus within *idd3*, lower IL-2 production by acutely activated T cells, and a lower proportion of Tregs relative to the diabetes-resistant NOD.*idd3*$^{b/b}$ congenic mouse. This assignment is consistent with the importance of IL-2 as a key trophic factor for Tregs (36). In contrast, here, the *idd3* region appears to have no influence on thymic generation of Tregs. Together, these results suggest that different genetic elements control different stages of Treg biology, a notion supported by the observation that the NOD/Bg7 differential is greater in the thymus than in the periphery. This dampening of the primary selection difference may reflect independent influences on Treg homeostasis in peripheral lymphoid organs that could partially readjust the level of circulating Tregs. Thus, the molecules encoded by the genetic loci on *Chr1* and *Chr11* that control Treg selection are probably followed by further homeostatic regulators of Treg numbers, perhaps through limiting cell–cell contacts or production of cytokines such as IL-2/21 or TGF-β. Indeed, TGF-β influences the survival and homeostasis of Tregs in the periphery, but not their generation in the thymus (37). As often seen for multigenic traits, the combination of alleles fixed in the NOD genome may balance the effect of lower IL-2 production by a higher thymic output, promoted by other genetic elements.

The *Chr1* and *Chr11* intervals were examined for candidate genes that might be associated with selection into the Treg lineage. FoxP3 itself (encoded on *ChrX*) is not a candidate. However, several genes that belong to the Treg signature are located on *Chr1*. *Rgs1* and *Rgs16*, which encode regulator-of-G protein signaling proteins and act as GTPase-activating proteins for Gα subunits, fine-tune cellular responses to chemokines (38). Indeed, Rgs16 is known to attenuate signaling by chemokine receptors in T lymphocytes (39). Different sensitivity to intrathymic chemokines could underlie differences in thymocyte trafficking and could perhaps influence Treg generation. *Mgat5* encodes a mannoside acetylglucosaminyltransferase that modulates responses to cytokines or TCR engagement with an enhanced susceptibility to autoimmunity in deficient mice (40). *Slamf1* encodes the signaling-lymphocyte-activation molecule (Slam, CD150) found on the surface of T cells and antigen-presenting cells (APCs). It is thought to play an important role in adhesion between T cells and APCs and has been shown to act as a coreceptor in TCR-dependent responses (41). Interesting, in T cells, SLAM-initiated signal transduction is in part controlled by SLAM-associated protein (SAP). An important function in immunobiology was attributed to SLAM and related receptors because mutations in SAP cause a severe immunodeficiency termed X-linked lymphoproliferative syndrome (41, 42). No obvious candidates stood out on the *Chr11* interval.

But then, if Treg selection is actually more efficient in NOD mice, why do these develop an autoimmune phenotype? One potential explanation is that the distribution of autoreactive TCRs is not the same in NOD and other strains. Because the optimal induction of Tregs occurs at a higher window of peptide concentration (or affinity) in the NOD than in the B6 thymus, self-antigens expressed at low levels in the NOD thymus may fail to deviate self-reactive T cell clones into the Treg lineage, having these autoreactive specificities to emerge peripherally on conventional T cells. Finally, it may simply be that the major problem in NOD mice is their defective central tolerance (28, 43), and that their Treg compartment, is ultimately unable to hold back the autoimmune potential unleashed in the thymus.

Materials and Methods

Mice. NOD/LtDOI (NOD), C57BL/6.*H2g7* (B6.H2g7or Bg7), and BDC2.5 TCR trangenic mice (26) on the NOD and B6.*H2g7* background (BDC2.5/NOD and BDC2.5/Bg7, respectively) were bred in the specific pathogen-free facility at the Joslin Diabetes Center or purchased from The Jackson Laboratory. NOD.*idd3*$^{b/b}$ congenic mice were purchased from Taconic (Rockville, MD). The BDC2.5/B6.H2g7 line was maintained by breeding trangenic B6.*H 2g7/b* MHC heterozygotes (BDC2.5/B6.H2g7/b) with B6.H2g7 to avoid genetic drift caused by early onset diabetes. Timed-pregnant females were obtained by mating mice overnight and separating the females in the morning (day of separation = day 0).

FTOC. Fetal thymus lobes were dissected from E15.5 embryos. Organs were cultured on sponge-supported filter membranes (Gel Foam surgical sponges; Amersham Pharmacia, Piscataway, NJ; Supor 450 membrane, 0.45-μm pore size, Pall Gelman Laboratory, East Hills, NY) at an interphase between 5% CO_2-humidified air and RPMI medium 1640 (10% FCS/50 μM 2-mercaptoethanol/2 mM L-glutamine/10 mM Hepes/nonessential amino acids/sodium pyruvate/penicillin/streptomycin). For negative selection experiments, FTOCs were supplemented with a BDC-specific peptide mimotope at indicated concentrations (BDCmi, peptide 1040–63; ref. 44). Medium/peptide was changed after 3 days of culture.

Repopulation Thymus Organ Culture. For repopulation experiments, thymus lobes were removed from E15.5 embryos and cultured on sponge-supported filters for 5 days in complete culture medium in the presence of 1.35 mM 2-deoxyguanosine. After culture, lobes were washed overnight by immersion in 50 ml of culture medium (without 2-deoxyguanosine) at 37°C, before repopulation with DN thymocytes from E15.5 embryos. Repopulation was obtained in Terazaki plates, incubating thymus lobes (one lobe per well) in hanging drops with $2–8 \times 10^5$ sorted DN cells for 12 h. Repopulated lobes were cultured on filters for 7 days, and then cells were harvested for FACS analysis.

Genetic Analysis. DNA was isolated from (B6.H2g7 $\times$ NOD) F_2 embryos and genotyped for SNP markers distinguishing B6 and NOD alleles by using 106 sets of *Taq*Man primers and probes (Assays by Design; Applied Biosystems, Foster City, CA) developed from the GNF database (http://snp.gnf.org) or NOD BAC end sequences (www.sanger.ac.uk/Projects/M_musculus-NOD). SNP markers covered all 19 autosomes and *Idd* loci with an average spacing of ≈25 Mb. The full list of primer/probe sets along with specific genomic locations (Mb positions based on the latest version of the National Center for Biotechnology Information genome assembly) can be accessed in SI Table 2). Genotyping reactions were carried out in 384-well plates by using 5-μl reaction volumes containing 8 ng of dehydrated genomic DNA and 2.5 μl of ABI Master Mix (2$\times$ concentrated), 900 nM of each primer, and 200 nM probes of each 2′-chloro-7′-phenyl-1,4-dichloro-6-carboxy fluorescein or 6-carboxy fluorescein-labeled probe. Standard *Taq*Man thermocycling conditions were followed, with endpoint fluorescence reads on an ABI 7900HT instrument and genotypes called with SDS software (Applied Biosystems). Genetic analyses were performed with R/qtl (45). Experiment empirical *P* values were established by permutation tests (10,000 permutations; R/qtl). QTLs were confirmed by using nonparametric interval mapping algorithms (R/qtl). 2D interval mapping for epistasis was performed by using R/qtl.

We thank Leilani Roser, Elzbieta Hyatt, and Kimie Hattori for assistance with mice and Joyce LaVecchio and Giridesh Buruzala for help with flow cytometry. This work was supported by Juvenile Diabetes Research Foundation Grant 4-2004-368, National Institutes of Health Grant 1R01DK60027, and Young Chair funds (to D.M. and C.B.) and Joslin's National Institute of Diabetes and Digestive and Kidney Diseases-funded Diabetes Endocrinology Research Care core facilities. M.F. was supported by Emmy-Noether Postdoctoral Fellowship FE 801/1-1 from the German Research Foundation and a Charles King Trust Postdoctoral Fellowship. W.J. was supported by the American Diabetes Association. P.H. was supported by the Cancer Research Institute.

1. Sakaguchi S, Ono M, Setoguchi R, Yagi H, Hori S, Fehervari Z, Shimizu J, Takahashi T, Nomura T (2006) *Immunol Rev* 212:8–27.
2. Khattri R, Cox T, Yasayko SA, Ramsdell F (2003) *Nat Immunol* 4:337–342.
3. Fontenot JD, Gavin MA, Rudensky AY (2003) *Nat Immunol* 4:330–336.
4. Hori S, Nomura T, Sakaguchi S (2003) *Science* 299:1057–1061.
5. Ziegler SF (2006) *Annu Rev Immunol* 24:209–226.
6. Fontenot JD, Rasmussen JP, Williams LM, Dooley JL, Farr AG, Rudensky AY (2005) *Immunity* 22:329–341.
7. Huehn J, Siegmund K, Lehmann JC, Siewert C, Haubold U, Feuerer M, Debes GF, Lauber J, Frey O, Przybylski GK, *et al.* (2004) *J Exp Med* 199:303–313.
8. Herman AE, Freeman GJ, Mathis D, Benoist C (2004) *J Exp Med* 199:1479–1489.
9. Jordan MS, Boesteanu A, Reed AJ, Petrone AL, Holenbeck AE, Lerman MA, Naji A, Caton AJ (2001) *Nat Immunol* 2:283–284.
10. Apostolou I, Sarukhan A, Klein L, von Boehmer H (2002) *Nat Immunol* 3:756–763.
11. Van Santen HM, Benoist C, Mathis D (2004) *J Exp Med* 200:1221–1230.
12. Liston A, Lesage S, Wilson J, Peltonen L, Goodnow CC (2003) *Nat Immunol* 4:350–354.
13. Fontenot JD, Dooley JL, Farr AG, Rudensky AY (2005) *J Exp Med* 202:901–906.
14. Chen W, Jin W, Hardegen N, Lei KJ, Li L, Marinos N, McGrady G, Wahl SM (2003) *J Exp Med* 198:1875–1886.
15. Apostolou I, von Boehmer H (2004) *J Exp Med* 199:1401–1408.
16. Anderson MS, Bluestone JA (2005) *Annu Rev Immunol* 23:447–485.
17. Salomon B, Lenschow DJ, Rhee L, Ashourian N, Singh B, Sharpe A, Bluestone JA (2000) *Immunity* 12:431–440.
18. Chen Z, Herman AE, Matos M, Mathis D, Benoist C (2005) *J Exp Med* 202:1387–1397.
19. Tarbell KV, Petit L, Zuo X, Toy P, Luo X, Mqadmi A, Yang H, Suthanthiran M, Mojsov S, Steinman RM (2007) *J Exp Med* 204:191–201.
20. Wu AJ, Hua H, Munson SH, McDevitt HO (2002) *Proc Natl Acad Sci USA* 99:12287–12292.
21. Alard P, Manirarora JN, Parnell SA, Hudkins JL, Clark SL, Kosiewicz MM (2006) *Diabetes* 55:2098–2105.
22. You S, Belghith M, Cobbold S, Alyanakian MA, Gouarin C, Barriot S, Garcia C, Waldmann H, Bach JF, Chatenoud L (2005) *Diabetes* 54:1415–1422.
23. Pop SM, Wong CP, Culton DA, Clarke SH, Tisch R (2005) *J Exp Med* 201:1333–1346.
24. Gregori S, Giarratana N, Smiroldo S, Adorini L (2003) *J Immunol* 171:4040–4047.
25. Bonasio R, Scimone ML, Schaerli P, Grabie N, Lichtman AH, von Andrian UH (2006) *Nat Immunol* 7:1092–1100.
26. Katz JD, Wang B, Haskins K, Benoist C, Mathis D (1993) *Cell* 74:1089–1100.
27. Gonzalez A, Katz JD, Mattei MG, Kikutani H, Benoist C, Mathis D (1997) *Immunity* 7:873–883.
28. Zucchelli S, Holler P, Yamagata T, Roy M, Benoist C, Mathis D (2005) *Immunity* 22:385–396.
29. Böhme J, Schuhbaur B, Kanagawa O, Benoist C, Mathis D (1990) *Science* 249:293–295.
30. Bogue MA, Grubb SC (2004) *Genetica* 122:71–74.
31. Romagnoli P, Tellier J, van Meerwijk JP (2005) *Eur J Immunol* 35:3525–3532.
32. Yamanouchi J, Rainbow D, Serra P, Howlett S, Hunter K, Garner VE, Gonzalez-Munoz A, Clark J, Veijola R, Cubbon R, *et al.* (2007) *Nat Genet* 39:329–337.
33. Cabarrocas J, Cassan C, Magnusson F, Piaggio E, Mars L, Derbinski J, Kyewski B, Gross DA, Salomon BL, Khazaie K, *et al.* (2006) *Proc Natl Acad Sci USA* 103:8453–8458.
34. Liston A, Lesage S, Gray DH, O'Reilly LA, Strasser A, Fahrer AM, Boyd RL, Wilson J, Baxter AG, Gallo EM, *et al.* (2004) *Immunity* 21:817–830.
35. Holler PD, Yamagata T, Jiang W, Feuerer M, Benoist C, Mathis D (2007) *Proc Natl Acad Sci USA* 104:7187–7192.
36. Fontenot JD, Rasmussen JP, Gavin MA, Rudensky AY (2005) *Nat Immunol* 6:1142–1151.
37. Marie JC, Liggitt D, Rudensky AY (2006) *Immunity* 25:441–454.
38. Moratz C, Hayman JR, Gu H, Kehrl JH (2004) *Mol Cell Biol* 24:5767–5775.
39. Lippert E, Yowe DL, Gonzalo JA, Justice JP, Webster JM, Fedyk ER, Hodge M, Miller C, Gutierrez-Ramos JC, Borrego F, *et al.* (2003) *J Immunol* 171:1542–1555.
40. Demetriou M, Granovsky M, Quaggin S, Dennis JW (2001) *Nature* 409:733–739.
41. Engel P, Eck MJ, Terhorst C (2003) *Nat Rev Immunol* 3:813–821.
42. Sayos J, Wu C, Morra M, Wang N, Zhang X, Allen, D., van Schaik S, Notarangelo L, Geha R, Roncarolo MG, *et al.* (1998) *Nature* 395:462–469.
43. Kishimoto H, Sprent J (2001) *Nat Immunol* 2:1025–1031.
44. Judkowski V, Pinilla C, Schroder K, Tucker L, Sarvetnick N, Wilson DB (2001) *J Immunol* 166:908–917.
45. Broman KW, Wu H, Sen S, Churchill GA (2003) *Bioinformatics* 19:889–890.